ISSN 0023-1584, Kinetics and Catalysis, 2009, Vol. 50, No. 5, pp. 691–704. © Pleiades Publishing, Ltd., 2009.
Original Russian Text © A.Ya. Rozovskii, M.A. Kipnis, E.A. Volnina, P.V. Samokhin, G.I. Lin, M.A. Kukina, 2009, published in Kinetika i Kataliz, 2009, Vol. 50, No. 5, pp. 718–733.

Laws of Selective CO Oxidation over a Ru/Al_2O_3 Catalyst in the Surface Ignition Regime: II. Transition States

A. Ya. Rozovskii†, M. A. Kipnis, E. A. Volnina, P. V. Samokhin, G. I. Lin, and M. A. Kukina

Topchiev Institute of Petrochemical Synthesis, Russian Academy of Sciences, Moscow, 119991 Russia

Received April 22, 2008

Abstract—The kinetics of selective CO oxidation (or individual CO or H_2 oxidation) over ruthenium catalysts are considerably as affected by the heat released by the reaction and specifics of the interaction of ruthenium with feed oxygen. In a reactor with reduced heat removal (a quartz reactor) under loads of ~70 l g_{Cat}^{-1} h^{-1} and reagent percentages of ~1 vol % CO, ~1 vol % O_2, ~60 vol % H_2, and N_2 to the balance, the reaction can be carried out in the catalyst surface ignition regime. When catalyst temperatures are below ~200°C, feed oxygen deactivates metallic ruthenium, the degree of deactivation being a function of temperature and treatment time. Accordingly, depending on the parameters of the experiment and the properties of the ruthenium catalyst, various scenarios of the behavior of the catalyst in selective CO oxidation are realized, including both steady and transition states: in a non-isothermal regime, a slow deactivation of the catalyst accompanied by a travel of the reaction zone through the catalyst bed along the reagent flow; activation of the catalyst; or the oscillation regime. The results of this study demonstrate that, for a strongly exothermic reaction (selective CO oxidation, or CO, or H_2 oxidation) occurring inside the catalyst bed, the specifics of the entrance of the reaction into the surface ignition regime and the effects of feed components on the catalyst activity should be taken into account.

DOI: 10.1134/S0023158409050115

Hydrogen is employed in fuel cells to produce electrical power; in this context, on-board hydrogen generators have a great potential [1].

Useful hydrogen sources are methanol, methane, and other hydrocarbon subjected to oxidative reforming to a hydrogen-rich gas. As a rule, the hydrogen-rich gas contains up to 1% CO. Carbon monoxide is poisonous to the platinum anodes of proton exchange membrane fuel cells. Its concentration in the reformate can be reduced to ~10 ppm by adding a small amount of air.

Efficient and selective (in the presence of hydrogen) catalysts of CO oxidation are catalysts based on Group VIII noble metals, in particular, ruthenium or Ru–Pt alloys [2–15]. Ruthenium catalysts, as a rule, have a temperature window of minimal residual CO levels with an upper bound below 200°C. Despite the large amount of work done in this field, data on the activity, stability, and optimal load of ruthenium catalysts are controversial.

Oh and Sinkevitch [2] compared ruthenium, rhodium, platinum, and palladium catalysts (Al_2O_3 supports; linear heating at 20 K/min; feed composition, vol %: CO, 0.09; O_2, 0.08; H_2, 0.85; N_2 to the balance; load: 20000 h^{-1}); these catalysts were arranged in the following decreasing order of CO oxidation activities: Ru ≈ Rh > Pt > Pd.

According to Han et al. [3], 5% Ru/Al_2O_3 catalyst is active in selective CO oxidation in the vapor/gas mixture modeling gases of steam methanol reforming and is efficient for a two-stage refining scheme. For a catalyst sample reduced at 150°C, for example, there is a temperature interval of 80–120°C where CO levels can be reduced from initial 2000 to 190–0 ppm, respectively. In long-term (1000-min) tests at 80°C, this catalyst noticeably loses activity.

Snytnikov et al. [4] studied supported ruthenium and platinum catalysts (Sibunit support, spheres 1–2 mm in diameter) containing 1 wt % metal. They used a flow quartz reactor 8 mm in diameter charged with 0.6 g of the catalyst mixed with 2 g of quartz. The effects of temperature and CO_2 and H_2O in the feed were studied in two feed compositions, vol %: CO, 1; O_2, 1.5; N_2, 23; H_2, 75.5; CO, 1; O_2, 1.5; CO_2, 20; H_2O, 3; H_2, 75.5; the flow rate was 0.3 g s cm^{-3}, or 12 l g^{-1} h^{-1}.

Snytnikov et al. [4] arrived at the following conclusions: the residual CO concentration has a temperature-dependent minimum; the temperature of this minimum for Ru/C is 30–40°C lower than for Pt/C. O_2 conversion increases with rising temperature to reach 100%; the conversion curve for Ru/C lies 30–40°C below that for Pt/C. Both for Ru/C and for Pt/C catalysts, the presence of CO_2 and H_2O in the feed increases the residual CO level but does not affect O_2 conversion. The minimal residual CO level can be

† Deceased.

reduced by increasing the O_2/CO ratio. In the presence of CO_2 over Ru/C catalysts, methane was detected at the outlet.

Thus, Ru/C is more active than Pt/C regardless of the presence or absence of CO_2 and H_2O. The catalytic stability of Pt/C and Ru/C catalysts was tested for 2 days at 160 and 110°C, respectively, on the feed composition, vol %: CO, 1; O_2, 1.5; CO_2, 20; H_2O, 3; H_2, 75.5. Both catalysts provided 100% O_2 conversion. Residual CO levels were 20 and 40 ppm, respectively, without noticeable deactivation of the catalyst.

Snytnikov et al. [4] thought that the reverse water–gas shift reaction occurs over Pt/C catalysts in the presence of CO_2:

$$CO_2 + H_2 = CO + H_2O. \quad (I)$$

Over Ru/C catalysts, this reaction occurs together with CO_2 hydrogenation to CH_4:

$$CO_2 + 4H_2 = CH_4 + 2H_2O. \quad (II)$$

Han et al. [5] did not observe any influence of water on oxidation over the 5% Ru/Al_2O_3 catalyst when up to 15 vol % water was added to an idealized reformate gas ($CO + H_2 + O_2$ mixture). According to Han et al. [3], however, H_2O positively affects the activity of the 5% $Ru/\gamma\text{-}Al_2O_3$ catalyst in selective CO oxidation in the presence of CO_2.

According to Echigo and Tabata [6], the 5% $Ru/\gamma\text{-}Al_2O_3$ catalyst reduced at 250°C demonstrates a high activity; this catalyst is prepared by impregnation of spherical alumina pellets 2–4 mm in diameter. For example, for the feed composition, vol %: CO, 0.5; O_2, 1.5; CO_2, 20; N_2, 6; H_2 to the balance, water percentage in the wet gas of 11 vol %, and volume flow rate of 7500 h^{-1} (calculated for the dry gas), the residual CO level was less than 7 ppm within 120–180°C. As temperature rises above 120°C, however, the methane percentage rises, too, in agreement with data for honeycomb ruthenium catalysts claimed in Patent WO/2003/080238 [10]. According to Han et al. [5], the 5% Ru/Al_2O_3 catalyst manifests its methanating activity above 200°C; the output methane level also increases with temperature elevation.

According to Kawatsu [7], the temperature interval where residual CO levels in the gas modeling methanol reformate can be reduced to 0 ppm for Ru/Al_2O_3 catalysts is 100–160°C for volume flow rates of 10000 and 15000 h^{-1}.

Xu Guangwen and Zhang Zhan-Guo [8] studied a commercial 0.5% Ru/Al_2O_3 catalyst in the linear heating regime (~1 K/min) with the load 45 l g_{Cat}^{-1} h^{-1}. The catalyst has a noticeable activity even at 345 K; above 463 K, the residual CO level drops to tens of ppm (gas composition, vol %: CO, 0.5; O_2, 0.3; H_2, 70.1; CO_2, 29.1). With this, the residual O_2 level drops to zero at 370 K. An increase in the O_2/CO ratio, though it raises the output methane levels, reduces the residual CO level. Xu Guangwen and Zhang Zhan-Guo conclude, with reference to the methanating activity of the catalyst, that the optimal temperature window for removal of CO is 383–423 K when the CO percentage in the feed gas is 1 vol % ($O_2/CO = 2.5$; load: ~5000 h^{-1}).

Dudfield et al. [9] proposed a two-stage 3.7-l reactor (a platinum–ruthenium catalyst is supported on alumina heat exchangers; Pt + Ru in each reactor is ~8.5 g). In the case of a typical gas of steam reforming of methanol (composition, vol %: H_2, 69.4; CO, 0.2–1.0; CH_3OH, 0.7; H_2O, 6.7; CO_2 to the balance), residual CO levels can be considerably reduced by properly selecting a temperature and the ratio O_2/CO for each stage. For example, for an initial CO level of 1 vol %, the overall ratio $O_2/CO = 3.5$ (air partition between reactors 1 and 2 is 2 : 1), and load of 300 l/min, the residual CO level is 6 ppm. The average temperature in the first reactor is 168°C; in the second reactor, 172°C.

Worner et al. [11] reduced residual CO levels to 30 ppm within 100–160°C over a honeycomb ruthenium catalyst (feed composition, vol %: H_2, 75; CO_2, 18; H_2O, 4; N_2, 2; CO, 0.4; O_2, 0.6; gas volume rate: 5000 h^{-1}).

For (0.5–1)% Ru/Al_2O_3 [12], there is a temperature window below 200°C where the residual CO level drops to 0 ppm (gas composition, vol %: H_2, 37; CO_2, 18; CO, 0.5; H_2O, 5; O_2, 1; He to the balance; gas flow rate: 67000 h^{-1}).

According to [13], in linear heating tests of a honeycomb ruthenium catalyst (heating rate: 10 K/min, flow rate: 60000 h^{-1}, initial CO percentage: 1 vol %), minimal residual CO levels in the dry gas (<10 ppm in the absence of methanol and <13 ppm for ~0 vol % methanol in the feed gas) are observed in the range 110–160°C.

Rosso et al. [14] inferred the preference of platinum catalysts for selective CO oxidation, because 1% Ru catalysts supported on zeolites A did not provide complete CO conversion without considerable methane formation: residual CO levels on a zeolite 5A supported catalyst were less than 10 ppm within 240–280°C, where methane formation is noticeable. Moreover, for the 1% Pt/zeolite 3A catalyst (264°C, $O_2/CO = 1.5$), a 10-ppm residual CO level was achieved even at a high flow rate (536000 h^{-1}).

Thus, the above literature survey makes it clear that most researchers study ruthenium catalysts at a GHSV of up to 20000 h^{-1}. For using fuel cells in automobiles, however, high loads in selective CO oxidation reactors are of interest. For a fuel cell with ~20 kW power, calculated flow rates are up to 400 l/min of the ~70% H_2 wet gas from steam reforming of methanol [9].

Accordingly, for the car power to be ~100 kW with the ~1-l catalyst volume, selective CO oxidation should occur at gas flow rates of at least 80 l g_{Cat}^{-1} h^{-1} (with ~50 vol % H_2 in the wet gas).

CO and H_2 oxidations are very exothermic reactions. In the course of reactions where the heat flux generated by the reaction starts to exceed the heat

release flux, the reaction can spontaneously enter the external diffusion region (Frank-Kamenetskii referred to this regime as catalyst surface ignition) with attendant spontaneous increases in temperature and conversion [16, 17].

We demonstrated that selective CO oxidation in a near-adiabatic flow reactor can enter the surface ignition regime and studied the features of this transition using modified (ruthenium-doped) [18, 19] and ruthenium [15] catalysts. When the reaction enters the surface ignition regime, a considerable temperature gradient appears across the catalyst bed, the position of the hot spot depending on the parameters of the experiment (load, feed composition, and heater temperature).

Over the 0.1 wt % ruthenium catalyst at a flow rate of ~90 l g_{Cat}^{-1} h^{-1}, residual CO levels of 10–15 ppm can be achieved; however, feed oxygen slowly deactivates the catalyst [15]. Deactivation decreases heat release by the reaction and, ultimately, quenches the catalyst surface.

The ruthenium deactivation by oxygen means that the current activity of a ruthenium catalyst, when studied in the linear heating regime, depends on the history of the sample [2, 8, 13].

Earlier [15] and in this work, we showed that oxygen can deactivate ruthenium up to ~200°C; therefore, it is necessary to check the inferences made in [3, 4, 6, 7, 11–13] that the upper bound of the temperature window of minimal residual CO levels lies below 200°C. (At the same time, the above literature survey reveals that temperature elevation above 200°C makes a certain problem for ruthenium catalysts because of possible methane formation.)

This work continues our investigations [15] into selective CO oxidation over ruthenium catalysts. Here, we examine various scenarios of catalyst performance in selective CO oxidation and in individual CO and H_2 oxidations including both steady and transition states; we have also studied the performance stability of catalysts containing 1, 0.1, and 0.04% ruthenium. Catalyst samples synthesized via ammonia precipitation (1% Ru samples) and adsorption impregnation from toluene solution (0.1% Ru samples) were studied earlier [15].

In what follows, we will demonstrate that the data gained and the analysis of the relevant literature are helpful to consider the general challenges of selective CO oxidation and to find routes to the efficient performance of catalysts based on group VIII noble metals.

EXPERIMENTAL

Reaction in a Nonisothermal Regime

Most catalytic experiments used a flow quartz reactor (5.5 mm in inner diameter) with a branch pipe for inserting thermocouples and a sealed-in filter for holding a catalyst sample (the scheme of the setup is found in [18]; its modification is in [15]).

Two Chromel–Alumel measuring thermocouples were inserted into the catalyst bed through the branch pipe using a ground-glass joint (the metallic housing was 1 mm in diameter). The thermocouples were embedded inside the catalyst bed 1–2 mm from the bed end (at the inlet and outlet).

Catalyst sample: weight, 0.21–0.23 g and bed height, 1.3–1.5 cm for the fraction 0.200–0.315 and 0.22 g and ~1.7 cm for the fraction 0.250–0.315 mm.

A multichannel processor (resolution: 0.1 K) was used for temperature control and measurement in the catalyst bed.

The temperature of the control furnace thermocouple was used as the test parameter for ascertaining the temperature of the gas entering the catalyst bed. (In the experiment with an alumina sample, the readings of the two measurement thermocouples, either both embedded into the bed or one mounted above the bed and the other inside the bed, differ only insignificantly from each other, differing from the furnace thermocouple readings by ~2.5°C at 110°C and ~7°C at 250°C.)

The gas flow rate was measured on an IRG-1000 digital flow meter and normalized to the STP (760 Torr, 0°C).

The gas leaving the reactor was separated into two streams. One stream was analyzed chromatographically for CO and O_2 (thermal-conductivity detector, zeolite 13X); the other (main) stream was directed to a BINOS 100 two-channel IR analyzer (in the CO channel, range: 0–9999 ppm; displaying resolution: 1 ppm; in CO_2 channel, range: 0–25 vol %; displaying resolution: 0.1 vol %). The analog output of the IR analyzer was connected to the input of the multichannel processor to provide the synchronous record of temperature, CO levels, and when required, CO_2 levels. For the 300 ml/min flow rate, the delay of the response of the IR analyzer relative to that of the thermocouples upon switching from hydrogen to the feed gas was ~0.5 min.

Before an experiment, the reactor was pressurized to check it for air tightness. A tilt valve was used for feed gas switching. After an experiment, the reactor was purged with hydrogen and the catalyst was left in a hydrogen atmosphere.

Stability of Catalyst Performance

For ascertaining the stability of catalyst performance, long-term operation of the catalyst was studied on a setup with a metallic reactor (modified KL-3D setup manufactured at the Design and Construction Bureau of the Institute of Organic Chemistry, Russian Academy of Sciences). In this reactor, a quartz-diluted catalyst was charged into an annular space between coaxially positioned steel tubes, which

Characteristics of the catalyst prepared

Sample	Synthesis procedure	Description of synthesis	Metal percentage, wt %	Size fraction, mm
1Ru	Adsorption impregnation	Support was flooded with an aqueous solution of $RuOHCl_3$, exposed for 20 h, and after water was decanted, dried at 120°C for 6 h	1	0.2–0.315
004Ru	Adsorption impregnation	As for sample 1Ru	0.04	0.25–0.315
1RuA	Precipitation with ammonia	As for sample 1Ru, but aqueous ammonia is added to pH 10 during impregnation	1	0.2–0.315
01RuT	Adsorption impregnation from toluene solution	Support was flooded with an organometallic complex dissolved in toluene; after 30-min stirring, solution was decanted. Drying as for sample 1Ru	0.1	0.2–0.315

were an insert into the reactor (~11 mm in diameter) and a thermocouple conduit (~4 mm in diameter). The catalyst sample was 0.22 g; quartz dilution was 1 : 3 (vol/vol). The entering feed flow in passing through the catalyst bed moved upward in the annular space between the insert and the inner wall of the reactor (the width of this space was 0.9 mm), which helped to level out the temperature profile across the catalyst bed with an inert. Hereafter, this reactor is referred to as isothermal.

The setup was equipped with a sampler for on-line chromatographic analysis of the vapor–gas mixture (chromatograph model 3700; column packed with Poropak T for water determination). Dried gases were analyzed on a Chrom 5 chromatograph (a column packed with Polisorb for CO_2 determination and a column packed with zeolite 13X for O_2, N_2, and CO determinations). Residual CO levels were determined on a BINOS 100 IR analyzer. The reactor pressure, as a rule, did not exceed 0.17 MPa.

O_2 and CO conversions were calculated from the surface areas of the relevant chromatographic peaks; small variations arising from H_2 and CO transformations were ignored.

The selectivity of O_2 consumption in CO oxidation was calculated from

$$S = 0.5C^0_{CO}X_{CO}/C^0_{O_2}X_{O_2}, \quad (1)$$

where X_{CO} and X_{O_2} are CO and O_2 conversions and C^0_{CO} and $C^0_{O_2}$ are initial CO and O_2 concentrations, respectively.

Feed Gas Mixtures

Feed gas mixtures were prepared in a preevacuated balloon with pressure monitored by a digital pressure gage. Commercially available H_2, CO_2, nitrogen were used; CO was generated by the decomposition of formic acid.

The CO channel of the IR analyzer was calibrated against mixtures prepared at the Balashikha Oxygen Plant; the CO_2 channel was calibrated against mixtures based on two gas streams (CO_2 and N_2) controlled by Bronkhorst flow regulators.

The error in CO concentration is determined by the uncertainties of calibration mixture compositions and the performance stability of the equipment. For low CO levels (~20 ppm), the CO determination error was not worse than 1–2 ppm.

Synthesis

The supports used were fractions of crushed commercial γ-Al_2O_3 extrudates (A-64k type, produced by the Ryazan Oil Refinery, 200 m^2/g surface area); before the active component was applied, the extrudates were calcined in air at 500°C for 2 h.

Table 1 lists the catalyst synthesis parameters and calculated metal concentrations. The starting ruthenium salt used was $Ru(OH)Cl_3$ purchased from the Aurat Plant, Moscow. The organometallic complex [20] prepared from this salt and triocrylamine was used to synthesize catalyst sample 01RuT (Table 1).

Once the catalyst was charged into the reactor, it was activated by reduction for 2 h in an H_2 flow (3.5 l/h) at 400°C (for sample 01RuT, at 350°C).

RESULTS

Depending on the history of the entrance of the catalyst into the reaction and the details of the experiment on ruthenium catalysts, various scenarios of the catalyst performance in selective CO oxidation (co or H_2 oxidation) can be implemented, including steady and transition states, as demonstrated by the results of the experiments below.

Effect of the Catalyst History on the Transition Regime

The steady-state surface ignition of an active catalyst (where oxygen conversion is ~100%) is acquired quite easily in a near-adiabatic reactor (a quartz reactor) under high loads.

For example, after heating the catalyst (sample 01RuT) in flowing H_2 and subsequent switching (Fig. 1a, 49th min) to the feed mixture (composition, vol %: CO, 0.93; O_2, 0.92; H_2, 62; N_2 to the balance; flow rate: 74 l g_{Cat}^{-1} h^{-1}), residual CO and O_2 levels at the reactor outlet drop rapidly to below 100 ppm (curves *1*, *2*); as soon as after ~12 min, the bed catalyst temperature reaches ~192°C instead of initial ~132°C (curves *4*, *5*). We think that the surface ignition regime is realized in this case.

During subsequent 50-min exposure, the bed outlet cools and the bed inlet slightly heats from 192 to ~195°C. This is due to the gradual localization of the reaction at the bed inlet and the associated change in the temperature of reactor walls in contact with the catalyst: heating in the reaction zone and cooling along the gas flow below the hot zone. Residual CO and O_2 levels reach ~2 and ~40 ppm, respectively, 1 h after the feed gas is admitted.

The behavior of the ruthenium catalyst in selective CO oxidation is considerably affected by the way in which the catalyst enters the operation regime, as demonstrated by the continuation of this experiment.

At the 114th minute (Fig. 1a), H_2 was admitted to the reactor, the furnace temperature lowered from 130 to 110°C, and then in the 147th minute, H_2 was replaced by the feed mixture. (Feed oxygen can deactivate ruthenium [15]; therefore, the reactor was purged with H_2 while temperature was lowered.) The admission of the feed mixture to the reactor did not result in noticeable O_2 and CO conversion: the catalyst is low active at this temperature. Then, H_2 admission to the reactor and its replacement by the feed mixture were repeated two times, with the furnace temperature increasing in steps (accordingly, H_2 was fed to the reactor in the 157th through 176th minute and in the 190th through 203rd minute; the feed was fed in the 176th through 190th min and then at the 203rd min). When the furnace temperature increased to 125°C, the O_2 and CO residual levels initially slightly decreased (203rd–219th min), but long-term exposure (for ~3 h at 125°C in the furnace) demonstrated a gradual deactivation of the catalyst (219th–377th min) and the accompanying rise in CO and O_2 residual levels (Fig. 1a, curves *1, 2*) and drop in bed temperature (Fig. 1a, curves *4*, *5*).

In what follows, we will demonstrate that, presumably, the trends of the CO and O_2 residual levels after 3-h-long exposure primarily reflect the systematic increase in the ruthenium surface coverage by adsorbed oxygen, which is responsible for the loss of the catalyst activity with time.

A rise in furnace temperature to 130°C (the furnace temperature is the same as by the 116th min) does not cause the system to enter the surface ignition regime, as did the replacement of H_2 by the feed mixture in the 49th min. This means that the catalyst activity became considerably lower.

The situation is changed radically only after the furnace temperature increases by another 5°C (400th min). In the first 20 min, the bed temperature increases abruptly, the residual CO level drops to less than 100 ppm (curve *1*), and the residual O_2 level decreases after passing through a peak (curve *2*). Further 1.5-h-long exposure causes the hot zone to move to the bed inlet and the residual reagent levels to decrease to ~50 ppm for O_2 and to ~2 ppm for CO.

Figure 1b illustrates more details of the alterations induced by rising furnace temperature from 130 to 135°C. Rising furnace temperature brings about a rise in catalyst temperature; first, the bed outlet temperature rises more rapidly than the inlet temperature to reach a maximum (~184°C) in the 417th minute. Then, the difference between the outlet temperature (Fig. 1b, curve *4*) and inlet temperature (Fig. 1b, curve *5*) decreases and, about the 437th min, the inlet temperature exceeds the outlet temperature: the hot zone has moved against the gas flow.

Thus, under the conditions of our experiments (i.e., for catalyst bed temperatures below ~180°C), depending on the chosen temperature of the outer heater, either the catalyst is deactivated or the catalyst partially deactivated by oxygen is gradually and spontaneously activated.

Effect of the O_2 Feed Level on the Entrance into the Surface Ignition Regime

The oxygen level in the feed, the flow rate of this feed, and the activity and selectivity of the catalyst in selective CO oxidation control the heat inflow into the reaction zone.

Figure 2 displays experimental data to illustrate the effect of the O_2 feed percentage on the performance of the 0.1% Ru/γ-Al_2O_3 catalyst (sample 01RuT). Switching at the 26th min from hydrogen to the feed composition, vol %: CO, 0.93; O_2, 0.92; H_2, 62; N_2 to the balance, at the furnace temperature 140°C induces the ignition of the catalyst surface, as in the experiment illustrated by Fig. 1.

Subsequent 20-min-long exposure brings about small changes in temperature and residual CO and O_2 levels. Following the catalyst activation by hydrogen (50th–66th min), the admission of a mixture with a lower O_2 percentage (composition, vol %: CO, 0.94; O_2, 0.52; H_2, 63; N_2 to the balance) does not lead to ignition (66th–112th min region). An initial drop in residual oxygen level (curve *2*) after some time changes to a rise. The residual CO level (curve *1*) has a similar trend. Accordingly, the catalyst temperature has a peak, the bed outlet being now hotter than the inlet. Thus, for this feed, the heat release from CO and H_2 oxidation is insufficient for the reaction to enter the catalyst surface ignition regime. Moreover, the catalyst activity systematically decreases because of deactivation by feed oxygen. It is only after a 30°C rise in furnace temperature and hydrogen activation (112th–

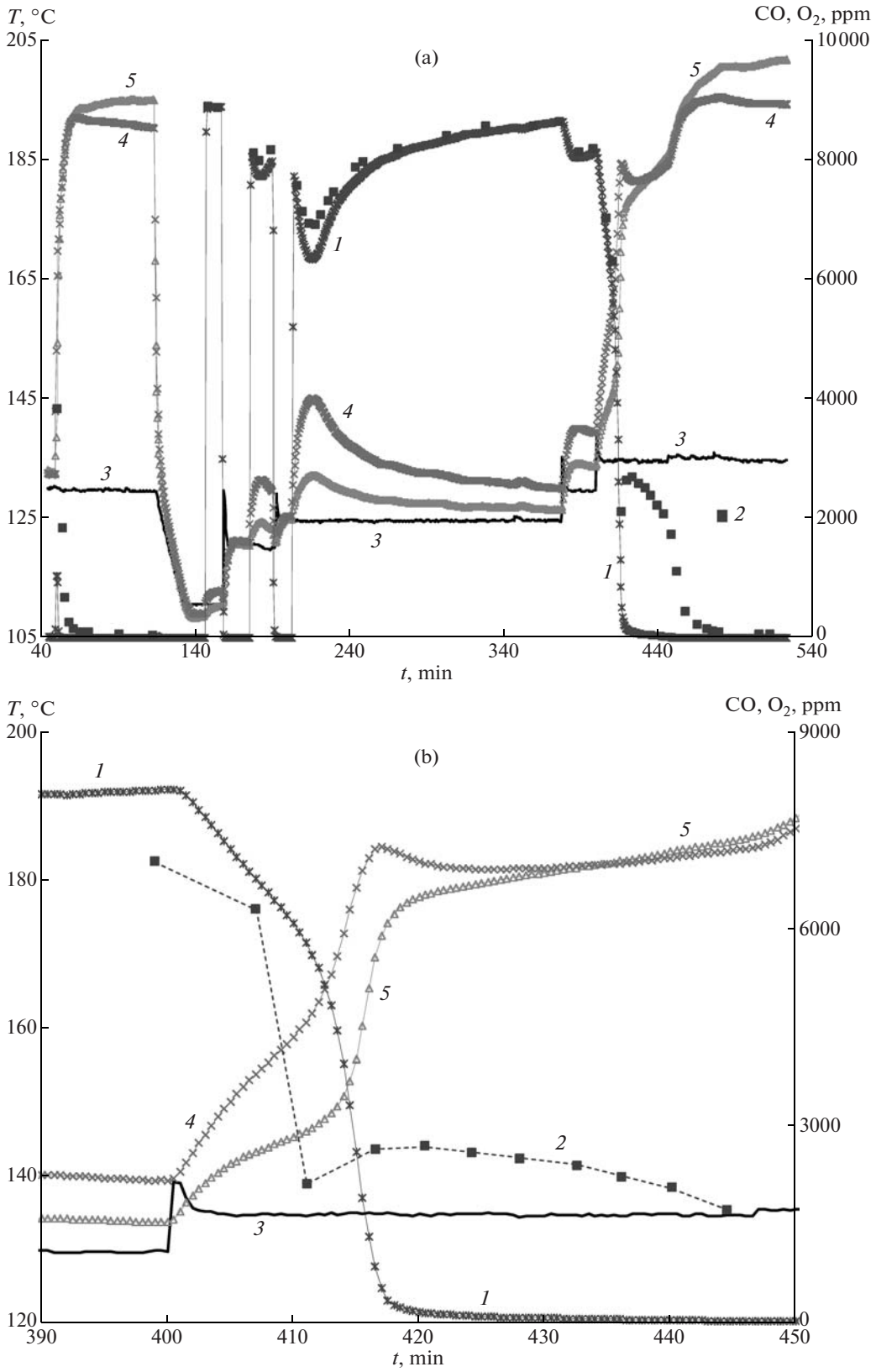

Fig. 1. (*1*, *2*) Residual (*1*) CO and (*2*) O_2 levels and (*3*–*5*) dynamics of (*3*) furnace temperature, (*4*) bed outlet gas temperature, and (*5*) inlet gas temperature (over catalyst sample 01RuT): (a) complete record and (b) a fragment. By the 49th min, 114th through 147th min, 157th through 176th min, and 190th through 203rd min, H_2 is fed to the reactor; in the other time, the feed composition, vol %, is CO, 0.93; O_2, 0.92; H_2, 62; N_2 to the balance. Feed flow rate: 74 l g_{cat}^{-1} h^{-1}.

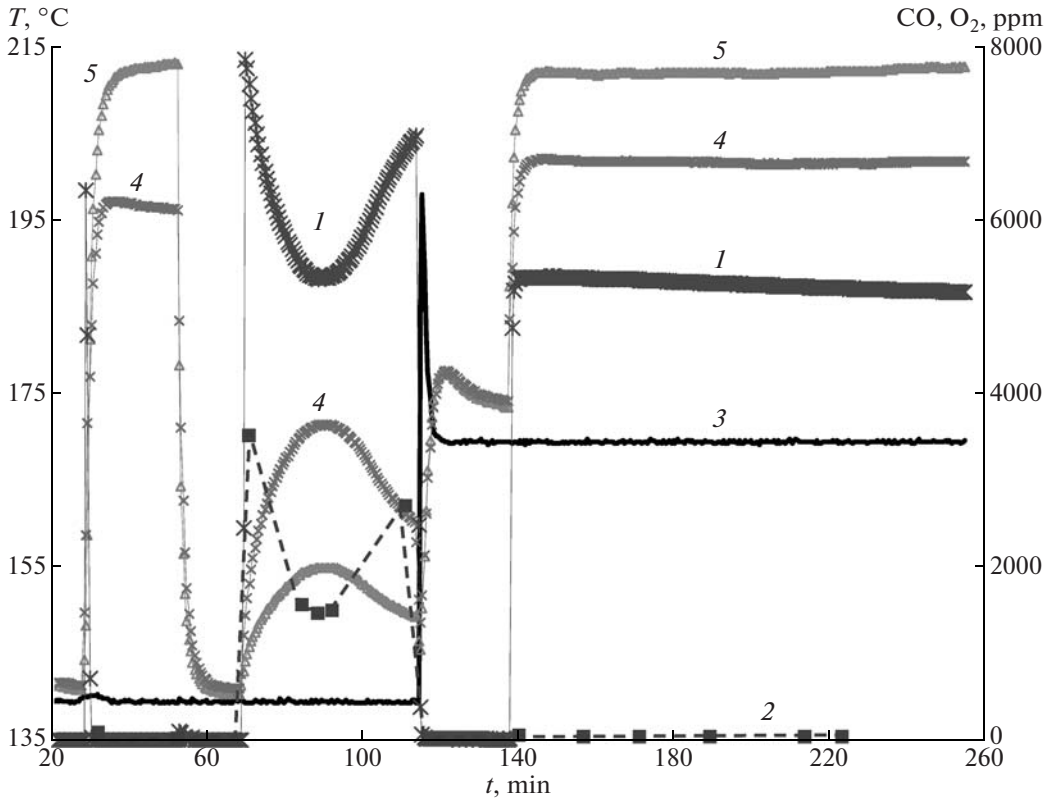

Fig. 2. (*1*, *2*) Residual (*1*) CO and (*2*) O_2 levels and (*3*–*5*) dynamics of (*3*) furnace temperature, (*4*) bed outlet gas temperature, and (*5*) inlet gas temperature (over catalyst sample 01RuT). By the 26th min, 50th through 66th min, and 112th through 136th min, H_2 is fed to the reactor; 26th through 50th min, the feed composition, vol %, is CO, 0.93; O_2, 0.92; H_2, 62; N_2 to the balance; 66th through 112th min and in the 136th min, the feed composition, vol %, is CO, 0.94; O_2, 0.52; H_2, 63; N_2 to the balance. Feed flow rate: 74 l g_{cat}^{-1} h^{-1}.

136th min) that the admission of the same feed (with a reduced oxygen percentage) causes ignition of the catalyst surface; the residual O_2 level drops to ~45 ppm (curve *2*). Exposure for ~2 h is accompanied by insignificant variations in temperature (curves *4*, *5*) and residual CO level (curve *1*), which is considerable (~5300 ppm) because of unoptimal oxidation parameters, primarily, the low ratio O_2/CO.

H_2 Oxidation

Figure 3 illustrates the temperature effect on H_2 oxidation over the 0.1% Ru/γ-Al_2O_3 catalyst. Following 0.5-h heating in a H_2 flow at 100°C, the catalyst was cooled to 44°C. At this temperature, the feed composition, vol %: O_2, 1; H_2, 60; N_2 to the balance, was admitted to the reactor. Oxygen conversion was not noticeable, and then the aforementioned feed was replaced by H_2 (the feed was admitted in the 194th min; H_2 was fed at the 203rd min; not shown in Fig. 3). Then, the feed and H_2 were fed alternately so that the feed was fed at a steady-state furnace temperature (in the 260th, 298th, 326th, and 354th min, respectively), whereas H_2 was fed before elevating furnace temperature (in the 269th, 308th, and 331st min, respectively). Each temperature rise (to 51, 61, or 71°C) induced a systematic small decrease in residual oxygen level (Fig. 3, curve *1*) and heating of the catalyst bed, primarily, at the outlet (Fig. 3; curves *3, 4*).

Lastly, the replacement of H_2 by the feed gas (at 354th min) while the furnace temperature was elevated from 71 to 81°C induced a strong drop in residual O_2 level (~40 ppm, 368th min) and a rapid rise in bed temperature, first at the outlet and then at the inlet (curves *3*, *4*). Thus, the reaction entered the surface ignition regime. Further 0.5-h exposure demonstrated slow bed temperature variations: a decrease at the inlet and an increase at the bed outlet (368th–404th min). In our opinion, these alterations (the movement of the hot spot from the bed inlet to outlet) are primarily associated with the slow deactivation of the catalyst by feed oxygen.

Performance Stability

The 0.1% Ru/γ-Al_2O_3 catalyst (sample 01RuT) was tested for steady performance in selective CO oxidation in a set of consecutive experiments (Fig. 4) in an

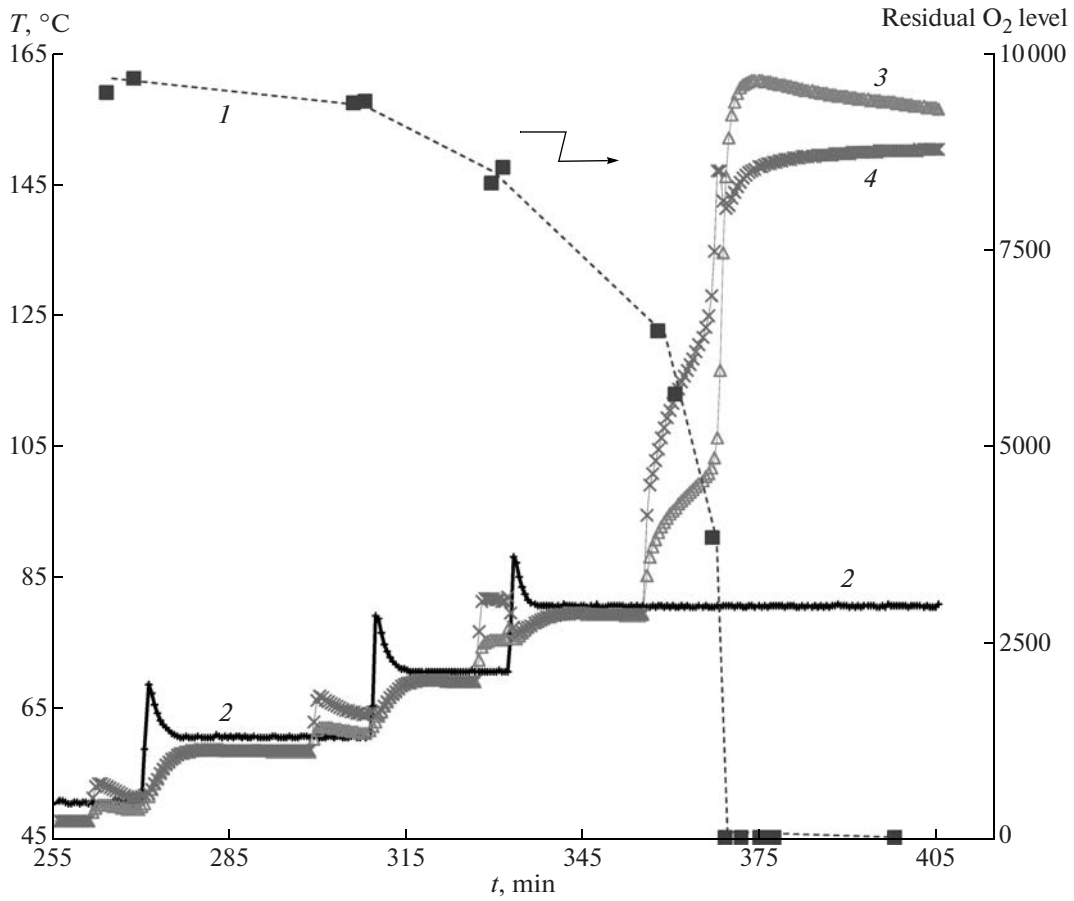

Fig. 3. Residual (*1*) CO level and (*2–4*) dynamics of (*2*) furnace temperature, (*3*) bed outlet gas temperature, and (*4*) inlet gas temperature (over catalyst sample 01Ru). Alternation of exposure of the catalyst in an H_2 flow and in a flow of composition, vol %: O_2, 1; H_2, 60; N_2, to the balance (by the 260th minute, an H_2 flow). Switch from H_2 to the feed gas, min: 260th, 298th, 326th, and 354th; reverse switch, min: 269th, 308th, and 311th, respectively. Feed flow rate: 75 l g_{cat}^{-1} h^{-1}.

"isothermal" reactor (feed composition, vol %: CO, 0.76; O_2, 0.76; CO_2, 18; H_2, 57; H_2O, 20; N_2 to the balance).

The freshly reduced catalyst was heated to 138°C in flowing H_2, after which the feed mixture was admitted to the reactor. The admission gave rise to an initially rapid and then slow increase in residual CO level for 5 h (curve *1*). After the catalyst was cooled in flowing H_2 to room temperature and the experiment was repeated, the residual CO level trend was reproduced (curve *2*).

In subsequent experiments, the catalyst was cooled and heated to a required temperature in the dry feed gas and water was fed to the evaporator after the catalyst temperature reached 80°C. Curves *3–7* show residual CO level trends. Inasmuch as in these experiments the catalyst was heated from room temperature in the feed gas, each curve has an initial tail starting at high CO values and reflecting the increase in CO conversion upon heating.

The superposition of the residual CO level curves so that the end of the preceding segment (138°C exposure) coincides with the onset of the following segment at the same temperature, allows the observation of a slow, long-term deactivation of the catalyst (the dashed trend in Fig. 4).

Assuming that deactivation arises from the oxidation of metallic ruthenium, we carried out three reduction cycles after 27.5-h-long operation: the catalyst operated being reduced in hydrogen first at 347°C for 2 h, then at 424°C for 3 h, and lastly, at 441°C for 4 h. Once reduced, the catalyst was cooled to 138°C in hydrogen, followed by the replacement of H_2 by the feed mixture. Figures 4 and 4a (curves *8–10*) show the relevant residual CO level curves in tests after each reduction. Figure 4a compares the residual CO trends over initial record segments for cycles with prereduction (initial segments were taken within 5–35 min, because up to the ~5th min, the curves reflect the transition regime that corresponds to a switch from the feed gas to H_2). Reduction at 347°C insignificantly increases the catalyst activity (Fig. 4a, curve *8*). A noticeable rise in activity is observed only after reduction at 424 and 441°C (curves *9, 10*), although the

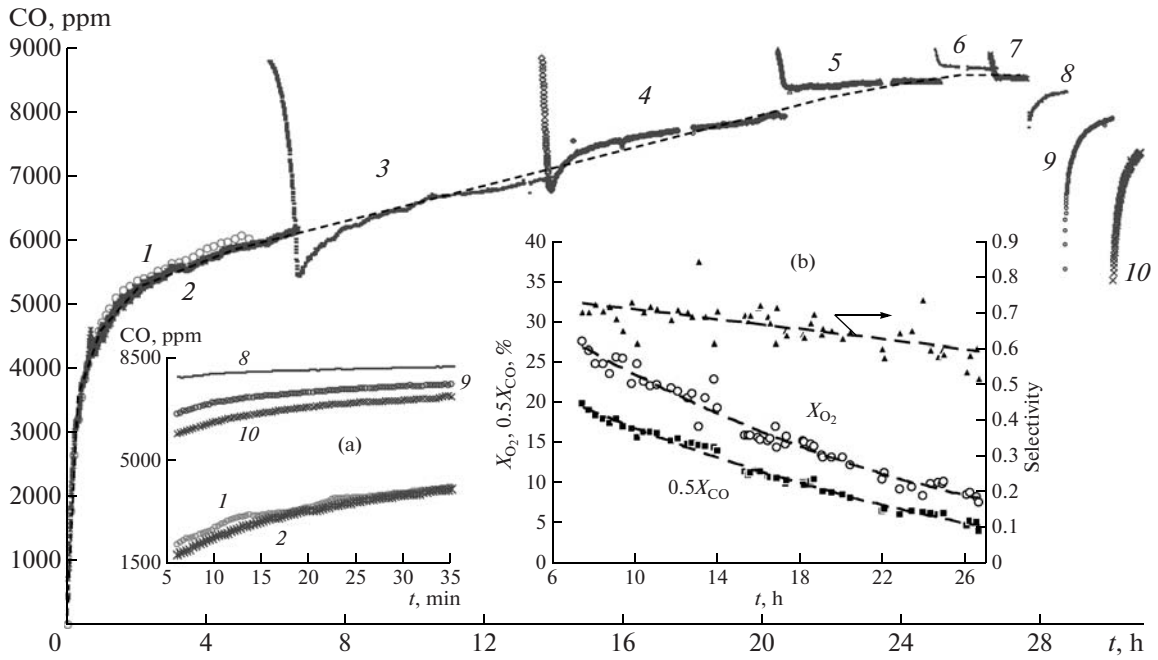

Fig. 4. Dynamics of residual CO level, CO and O_2 conversion, and selectivity of selective CO oxidation in an isothermal reactor at 138°C (over catalyst sample 01RuT). Panel (a): (*1*, *2*, *8–10*) initial record segments. Panel (b): dynamics of CO half-conversion ($0.5X_{O_2}$), O_2 conversion (X_{O_2}), and selectivity. Feed composition, vol %: CO, 0.76; O_2, 0.76; CO_2, 18; H_2, 57; H_2O, 20; N_2 to the balance. Flow rate: 30 l g_{cat}^{-1} h^{-1}. The catalyst is heated from room temperature to 138°C in (*1*, *2*) H_2 and (*3–7*) the feed gas mixture. Cooling: (*8–10*) from the activation temperature to 138°C in H_2. Catalyst sample size: 0.22 g with quartz dilution 1 : 3 (vol/vol).

residual CO level still tends to increase and considerably exceeds the residual CO level over the fresh catalyst (curves *1*, *2*). Noteworthy, the CO level in the feed is 9500 ppm (calculated for the dry gas). On the fresh catalyst after 0.5-h performance, the residual CO level was ~4000 ppm (Fig. 4a; curves *1, 2*), whereas after 27.5-h-long operation and reduction cycles, the respective values were 8200, 7600, and 7200 ppm (Fig. 4a; curves *8–10*).

Figure 4b displays CO and O_2 conversion data and selectivity as a function of operation time. Characteristically, the O_2 conversion curve, although lying above the CO half-conversion curve, does not exceed it by more than 1.5 times. The CO and O_2 feed levels being identical, according to (1) this means that CO oxidation selectivity is higher than 0.5 over the entire test period, which is supported by the relevant curve (Fig. 4b). Interestingly, selectivity decreases only insignificantly in the course of operation from ~0.7 in the beginning to ~0.6 in the end of the experiment, despite considerable alteration of the state of the catalyst.

Thus, during long-term operation the catalyst experiences partial deactivation and associated serious structural alterations.

Oscillatory Regime

Under conditions that favor both ruthenium oxidation by oxygen and the entrance of the reaction into the surface ignition regime, H_2 and CO oxidation reactions can occur while the catalyst activity changes with time, which gives rise to oscillations.

Figure 5 displays the results of CO oxidation experiments in the absence of hydrogen. The catalyst (sample 1RuA) was heated to 155°C (the furnace temperature) for 30 min in the feed gas of composition, vol %: CO, 0.88; O_2, 0.85; N_2 to the balance; as a result, both the residual CO level (0 ppm, 32nd–47th min, curve *1*) and the residual O_2 level (~4200 ppm at 32nd min, curve *2*) dropped and the catalyst heated (maximally to 194°C at the inlet and to 202°C at the outlet). The phenomena observed can be interpreted as catalyst surface ignition. However, the surface ignition state was not steady. Starting at the 40th min, temperature rapidly drops first at the bed inlet and then at the outlet, and the reaction is quenched. Accordingly, the residual CO level increases abruptly at the 47th min.

The 5°C rise in furnace temperature in the 56th min repeated the situation: rapid ignition was followed by rapid quench (56th–97th min).

However, subsequent long-term exposure at a fixed furnace temperature leads to a slow decrease in resid-

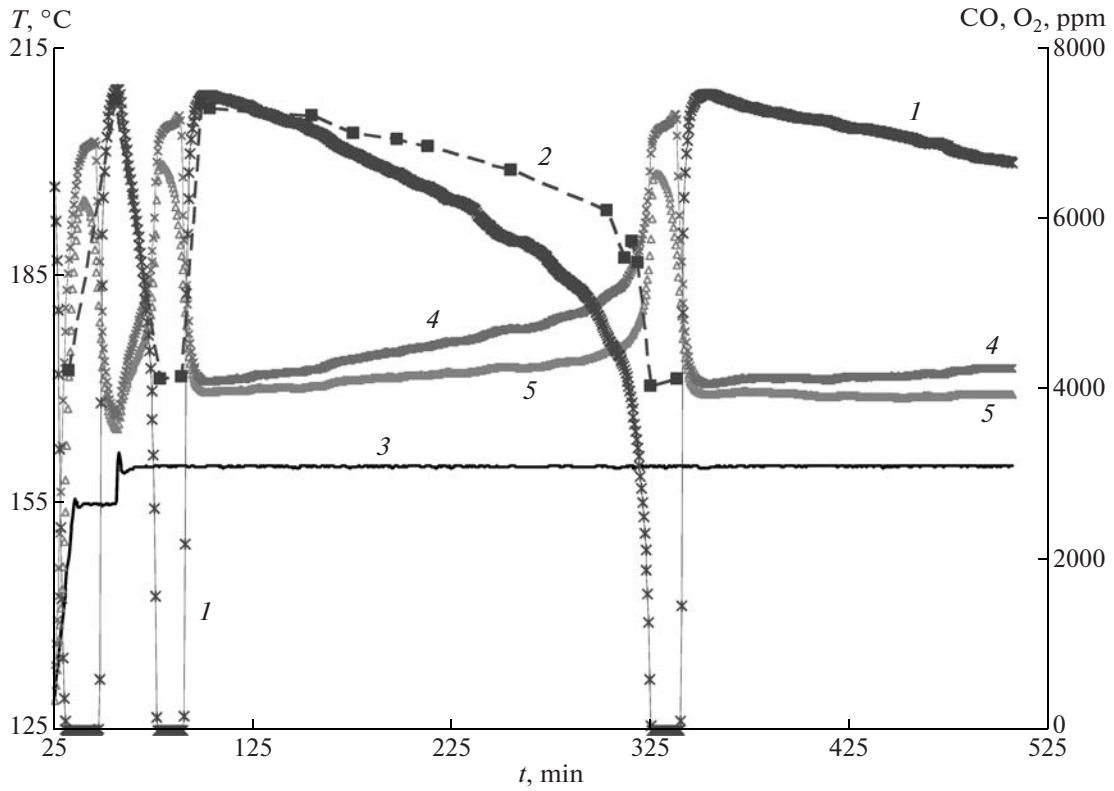

Fig. 5. Spontaneous oscillations during selective CO oxidation (over the catalyst sample 1RuA): (*1*, *2*) residual CO and O_2 levels, (*3*) furnace temperature, (*4*) bed outlet gas temperature, and (*5*) inlet gas temperature. Feed composition, vol %: CO, 0.88; O_2, 0.85; N_2 to the balance. Flow rate: 80 l g_{cat}^{-1} h^{-1}.

ual O_2 level with a concurrent decrease in residual CO level and a rise in catalyst temperature (at ~100th min). The decreasing rates of the residual reagent levels increase in response to the increase in catalyst bed temperature induced by spontaneous heating of the catalyst; ultimately, the catalyst is rapidly heated, the residual CO level drops to ~0 ppm, and the residual O_2 level drops to ~4000 ppm (in the 325th min). Thus, CO oxidation lasts until it is completely exhausted; the reaction enters the surface ignition regime. This state of the catalyst is unsteady; over ~12 min, the catalyst temperature rapidly decreases and the residual CO level abruptly increases. Characteristically, the decrease of the catalyst temperature at the bed inlet is such that, in the 330th through 337th min, the bed inlet and outlet temperatures have opposite trends: the hot zone moves toward the bed outlet. Then, over ~15 min, the catalyst is cooled because of surface quenching, which is again followed by a spontaneous slow heating of the catalyst and an associated systematic decrease in residual CO level.

Thus, the slow rise in catalyst activity that leads to surface ignition goes in hand with a rapid deactivation period.

The appearance of oscillations in selective CO oxidation (in the presence of H_2) is illustrated by an experiment on the 0.04% $Ru/\gamma\text{-}Al_2O_3$ catalyst (sample 004Ru) (Fig. 6). The catalyst was heated in flowing H_2 to the 250°C furnace temperature. Then, H_2 was replaced by the feed gas of composition, vol %: CO, 0.93; O_2, 0.92; H_2, 62; N_2 to the balance. After the feed gas was admitted and the temperature was decreased for the steady furnace temperature of 169°C, oscillations appeared (180th–570th min) in residual reagent (CO and O_2) levels at the reactor outlet (curves *1*, *2*), residual product (CO_2) level (curve *6*), and bed temperature (curves *4*, *5*). The length of the oscillation period was ~1 h; the oscillation amplitude tended to increase.

DISCUSSION

Surface Ignition and Quenching Features in the Catalyst Bed

We quite comprehensively considered surface catalyst ignition as a heterogeneous reaction in [18]; some features of this phenomenon related to an extended catalyst bed are considered in [15].

The catalyst bed enters the surface ignition regime and exits from this regime once a certain *critical* (ignition or quenching, respectively) *temperature* in the hot spot of the catalyst bed is reached.

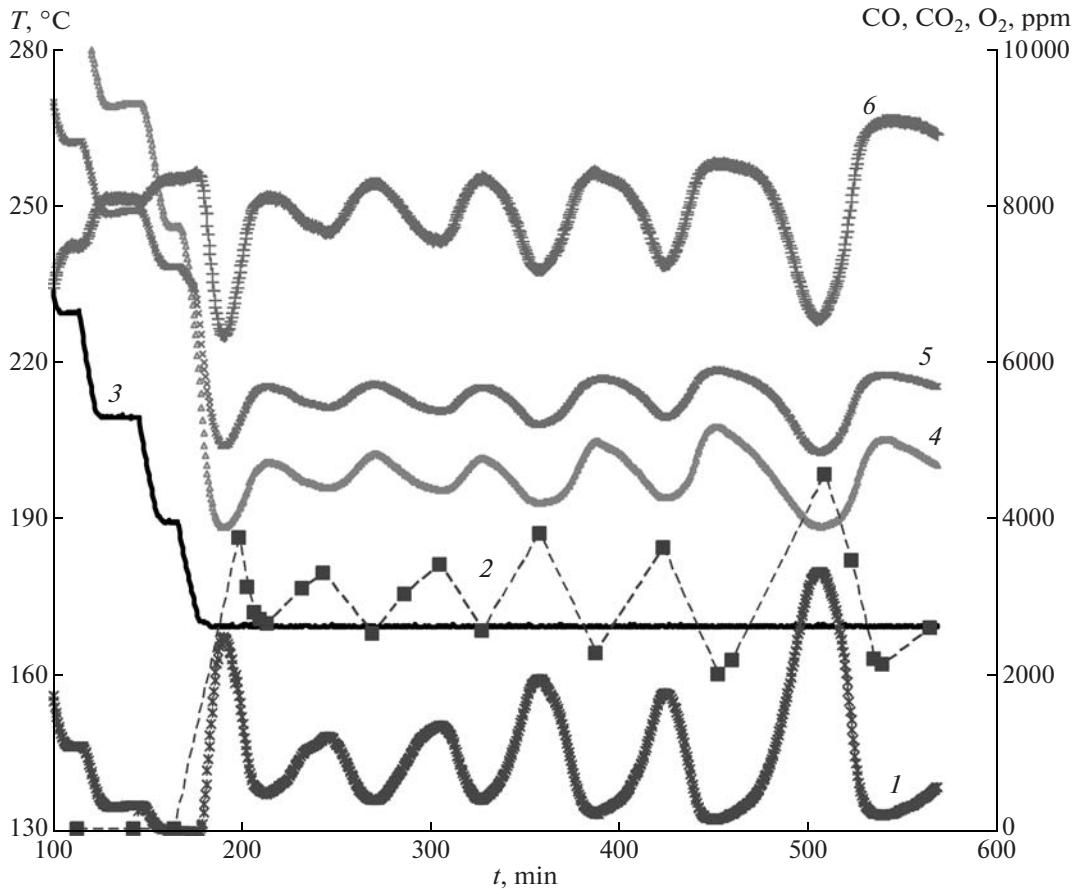

Fig. 6. Spontaneous oscillations during selective CO oxidation (over catalyst sample 004Ru): (*1*, *2*) residual CO and O_2 levels, (*3*) furnace temperature, (*4*) bed outlet gas temperature, (*5*) inlet gas temperature, and (*6*) CO_2 concentration. Feed composition, vol %: CO, 0.93; O_2, 0.92; H_2, 62; N_2 to the balance. Flow rate: 76 l g_{cat}^{-1} h^{-1}.

The critical ignition temperature decreases with decreasing the contribution of the reactor to heat removal. Heat removal through and along walls in a quartz reactor is lower than in a metallic one; accordingly, the reaction more easily enters the ignition regime in a quartz (adiabatic) reactor. On the other hand, the critical ignition temperature should increase in response to a decrease in the key component levels, an increase in the heat capacity of the feed, and dilution of the catalyst by an inert; the dilution increases the contact area between the bed and walls of the reactor and increases heat release through the walls.

The critical ignition temperature also decreases with decreasing catalytic activity. Evidently, the initial catalyst activity can be controlled via varying synthesis parameters.

Similar considerations also pertain to the critical quenching temperature.

Before ignition and in the initial moment of the transition regime, the hot spot is at the outlet from the catalyst bed. The entrance into the steady-state ignition regime is accompanied by the travel of the hot spot against the feed flow. However, if there is any factor influencing the catalyst activity at various spots of the bed (e.g., deactivation; see above), this would affect the character of entrance to the surface ignition regime in response to rising temperature (see, e.g., Figs. 1a, 1b).

If the hot spot was at the bed inlet, upon quenching it starts to travel against the feed flow to the boundary of the bed. Both in ignition and quenching, the transition regime generates a traveling zone inside the catalyst bed where the reaction occurs in the external diffusion regime; in the case of ruthenium, the specifics of its interaction with the feed oxygen also influence the character of the transition regime.

Under steady-state surface ignition, the reaction occurs in the external diffusion region; therefore, variations within certain bounds of temperature and flow rates do not induce quenching of the reaction.

This gives rise to a hysteresis in reagent conversion or catalyst temperature as a function the outer heater temperature (the temperature of the feed entering the reactor). We demonstrated the possibility of a hystere-

sis in selective CO oxidation for a modified platinum (ruthenium-doped) catalyst [15, 19].

Many researchers observed catalyst surface ignition and quenching in very exothermic reactions, in particular, CO oxidation.

A hysteresis was observed in CO oxidation upon stepwise heating/cooling over Pd/NaZSM-5 [21], Ru/SiO_2 [22], and Rh/SiO_2 [23] catalysts; on honeycomb platinum catalysts in the linear heating/cooling regime [24, 25]; and upon stepwise increase/decrease of O_2 concentration in the feed [25, 26]. Temperature hysteresis in CO oxidation and methanation was observed in [27] (in [15], we discussed the interpretation given to the hysteresis in that work).

Although hysteresis [21–26] and jump in CO conversion in response to a small variation in temperature in selective CO oxidation over a platinum [28] or rhodium [29] catalysts were related by the authors of those works to ignition, possible variations in the temperature profile of the catalyst bed and their effects on the phenomena observed are, as a rule, ignored.

While the reaction temperature for selective CO oxidation over a 1% Ru catalyst in [6] was set equal to the bed inlet temperature, in [2] the catalyst temperature was set equal to the temperature of the middle of the bed, although the axial temperature gradient in the catalyst bed reached 15°C. In [12, 14], the control thermocouple of the furnace was embedded into the catalyst bed (sample size: 0.15 g; bed height: 2 cm), although for a GHSV of 67000 h^{-1} and oxygen percentage of 1 vol %, considerable heat evolution should be observed and, as a consequence, the furnace performance should depend on the position of the hot spot inside the bed.

Practical implementation of the surface ignition regime is exemplified by ammonia oxidation [30, 31]. A large-scale ammonia oxidation reactor performs so that the reaction occurs inside the front layer of platinum grids with the layer thickness being as small as ~5 mm. "The reaction is accompanied by vigorous heat release, goes at a very high rate, and completes in about 1 ms or even sooner" [30, p. 272]. Ammonia oxidation under high loads leads to vigorous heat release: the working catalyst temperature is ~900°C, although in the case of platinum, the reaction is ignited at a relatively low temperature of 150–180°C [31].

Thus, the behavior of the catalyst under noticeable heat release by the reaction cannot be understood unless using data on the behavior of the entire catalyst bed under the reaction conditions.

Role of Oxygen

Oxygen plays a dual role in the ruthenium catalysts of CO oxidation. On the one hand, heat release as a result of CO and H_2 oxidation is proportional to the unreacted oxygen amount; in the steady-state surface ignition regime, oxygen is almost completely exhausted. The decreasing feed oxygen percentage increases the critical ignition temperature (Fig. 2). On the other hand, once oxygen occurs over a reduced catalyst, it can deactivate metallic ruthenium, the degree of deactivation being a function of temperature and treatment time so that long-term deactivation results in deep ruthenium oxidation (Fig. 4). At the same time, even though oxidized, ruthenium still has some selective CO oxidation activity (Fig. 4).

Accordingly, a combination of two time-variable factors is useful to understand the character of the phenomena observed over ruthenium catalysts, namely, heating up of the catalyst as a result of oxidation reactions and variations in catalyst activity as a result of ruthenium oxidation. With reference to literature data on deactivation of ruthenium catalysts by oxygen [3, 15, 22, 32, 33] and our data obtained in this work (Figs. 1–4), we infer that oxygen deactivation is significant for catalyst temperatures lower than ~200°C. Accordingly, at lower temperatures, partially oxidized ruthenium catalysts can be operative in selective CO oxidation.

(We should mention that Cant et al. [32] observed a decrease in catalyst activity during 7.7 h for the ratio $O_2/CO = 4.5$, whereas for $O_2/CO = 1.8$, several measurements during 22.5 h showed an increase in catalyst activity. From our data, the rise in catalyst activity can be due to the slow entrance of the reaction into the ignition regime; see Fig. 5.)

Let us proceed with considering the role of oxygen in selective CO oxidation in the steady-state surface ignition regime. Earlier [15] we demonstrated for ruthenium catalysts in the steady-state surface ignition regime that temperature depression does not influence the residual O_2 level (which is less than 100 ppm), but considerably influences the residual CO level (the results were obtained for the feed gas ratio $O_2/CO = 1$). We observed the same trend for rhodium catalysts. This implies that oxygen is the key component that governs the entrance of the reaction into the external diffusion region with an excess of oxygen relative to CO.

Specific Features of Catalysts Associated with the Metal Type

Goodman et al. [34] in their survey analyzed the behavior of ruthenium catalysts in CO oxidation. They noted that ruthenium differs from the other Group VIII metals. For platinum, palladium, and rhodium, characteristic is strong CO adsorption on metal surfaces, whereas ruthenium, depending on oxygen partial pressure and temperature, can react with the surface oxygen coverage to form bulk oxygen-containing structures until RuO_2 is formed.

The character of the interactions of ruthenium, platinum, and rhodium with CO and O_2 is the same in selective CO oxidation (for ruthenium, we demon-

strate this here; for platinum, see, e.g., [35]; for rhodium, our data will appear later elsewhere).

Thus, while for platinum and rhodium catalysts, increasing O_2/CO ratios should decrease residual CO levels and improve the stability of performance, for ruthenium catalysts, on the contrary, deactivation is expected.

Transition States and Oscillations

A combination of factors enhancing both ignition and deactivation gives rise to the oscillation behavior of CO oxidation (Figs. 5, 6).

We think that we are dealing with self-oscillations in CO oxidation (Fig. 5) [36].

The character of selective CO oxidation oscillations (Fig. 6), although differing from CO oxidation oscillations in the absence of hydrogen, likely has the same nature, and theoretical considerations should take in account H_2O oxidation.

Possibility of Side Reactions

Recall that selective CO oxidation can involve reverse gas–water shift reaction (reaction I) and methanation of carbon oxides, primarily, CO_2 (reaction II).

We also observed methane formation over the 1% $Ru/\gamma\text{-}Al_2O_3$ catalyst when selective CO oxidation occurred in the surface ignition regime [15]. In the same work we demonstrated that methane formation is reduced when temperature is depressed and the metal percentage decreases to 0.1 wt %.

If selective CO oxidation is carried out in the catalyst surface ignition regime so that the hot spot lies at the inlet to the catalyst bed, then the combination of feed components (namely, CO, H_2O, CO_2, and H_2) in lower lying sections of the reactor can thermodynamically favor reverse gas–water shift reaction (reaction (I)). For example, the hydrogen-containing feed gas for the water–gas shift reaction, which has been prepared by, for example, steam methanol reforming, can contain up to 20 vol % CO_2, whereas the CO level after oxidation in the front layer can decrease to ~100 ppm or even lower levels. This combination thermodynamically favors CO_2 reduction to CO. However, there are some factors that can inhibit this reaction. Selective CO oxidation can be carried out at high loads (short contact times). A decrease in contact time should reduce the rate of the reverse water–gas shift reaction. Temperature depression, which also becomes possible after selective CO oxidation enters the surface ignition regime, is also favorable in this context. Lastly, a decrease in the overall catalyst activity to the level suitable for the main reaction can also decrease the contribution of this side reaction to residual CO concentration.

CONCLUSIONS

The entrance of the reaction into the surface ignition regime is considered in [16, 17]. Rozovskii [16] compiled data on the synthesis of alcohols from CO and H_2 over fused iron catalysts. Frank-Kamenetskii [17] complied data on hydrogen and ammonia oxidation over a platinum wire. Unfortunately, the theoretical considerations in these works ignore the extent of the catalyst bed along the feed propagation.

Selective CO oxidation involves two concurrent reactions of CO and H_2 oxidation. On the one hand, more difficulties appear in the interpretation of the phenomena observed; on the other, the selectivity of the target reaction depends on a number of factors. For ruthenium catalysts, moreover, deactivation by oxygen comes into play. A considerable extent of the catalyst bed also adds some difficulties.

We studied all aforementioned features of selective CO oxidation in the surface ignition regime previously [15, 18, 19] and in this work.

While our previous works [15, 18, 19] demonstrated the possibility of selective CO oxidation entering the surface ignition regime and studied the specifics of this transition inside the catalyst bed, this work considers the specifics of the transition regime involving both catalyst surface ignition and ruthenium deactivation by oxygen.

Summing up the results, we come to the following conclusions. The entrance of the reaction into the surface ignition regime inside a catalyst bed starts with catalyst warming up at the bed outlet. Then, the reaction zone can propagate upward the bed, this propagation being limited by heat removal and catalyst activity in upper lying layers so that, in the steady state, the reaction zone can be displaced to the bed inlet. The surface ignition regime for ruthenium catalysts is steady unless the catalyst activity changes.

Inasmuch as oxygen participates in two reactions, temperature variations in the surface ignition regime allow the observation of the selectivity of oxygen consumption in the target reaction of CO oxidation.

The heat evolved during CO and H_2 oxidation reactions is roughly proportional (with account for the difference between the heats of the reactions) to the unreacted oxygen amount; thus, the oxygen consumption affects temperature distribution over the catalyst bed. On the other hand, below ~200°C oxygen deactivates metallic ruthenium; the degree of deactivation is a function of temperature and treatment time. Therefore, this dual role of oxygen makes understandable the phenomena observed in selective CO oxidation over ruthenium catalysts.

To summarize, the scenario of the operation of the catalyst in selective CO oxidation depends on the catalyst history and the parameters of the experiment: the reaction can occur in the steady-state surface ignition regime; slow deactivation of the catalyst is possible with a drop in activity (in a nonisothermal regime with

the movement of the reaction zone along the feed flow); in certain settings, the activation of the catalyst can be observed; and an oscillation regime is also possible.

The results of this study demonstrate that, given that a strongly exothermic reaction (selective CO oxidation or CO or H_2 oxidation) occurs inside the catalyst bed, the specifics of the reaction entrance into the surface ignition regime and the effects of feed components on the catalyst activity should be taken into account.

ACKNOWLEDGMENTS

This work was supported by the Russian foundation for basic research (project no. 06-03-32848).

REFERENCES

1. Pischinger, S., *Top. Catal.*, 2004, vol. 30/31, p. 5.
2. Oh, S.H. and Sinkevitch, R.M., *J. Catal.*, 1993, vol. 142, p. 254.
3. Han, Y.-F., Kinne, M., and Behm, R.J., *Appl. Catal., B*, 2004, vol. 52, p. 123.
4. Snytnikov, P.V., Sobyanin, V.A., Belyaev, V.D., Tsyrulnikov, P.G., Shitova, N.B., and Shlyapin, D.A., *Appl. Catal., A*, 2003, vol. 239, p. 149.
5. Han, Y.-F., Kahlich, M.J., Kinne, M., and Behm, R.J., *Appl. Catal., B*, 2004, vol. 50, p. 209.
6. Echigo, M. and Tabata, T., *Appl. Catal., A*, 2003, vol. 251, p. 157.
7. Kawatsu, S., *J. Power Sources*, 1998, vol. 71, p. 150.
8. Xu Guangwen and Zhang Zhan-Guo, *J. Power Sources*, 2006, vol.157, p. 64.
9. Dudfield, C.D., Chen, R., and Adcock, P.L., *J. Power Sources*, 2000, vol. 86, p. 214.
10. Patent WO/2003/080238.
11. Worner, A., Friedrich, C., and Tamme, R., *Appl. Catal., A*, 2003, vol. 245, p. 1.
12. Rosso, I., Antonini, M., Galletti, C., Saracco, G., and Specchia, V., *Top. Catal.*, 2004, vol. 30/31, p. 475.
13. US Patent 6 576 208.
14. Rosso, I., Galletti, C., Saracco, G., Garrone, E., and Specchia, V., *Appl. Catal., B*, 2004, vol. 48, p. 195.
15. Rozovskii, A.Ya., Kipnis, M.A., Volnina, E.A., Samokhin, P.V., and Lin, G.I., *Kinet. Katal.*, 2008, vol. 49, no. 1, p. 99 [*Kinet. Catal.* (Engl. Transl.), vol. 49, no. 1, p. 92].
16. Rozovskii, A.Ya., *Geterogennye khimicheskie reaktsii: Kinetika i makrokinetika* (Heterogeneous Chemical Reactions: Kinetics and Macrokinetics), Moscow: Nauka, 1980.
17. Frank-Kamenetskii, D.A., *Diffuziya i teploperedacha v khimicheskoi kinetike* (Diffusion and Heat Transfer in Chemical Kinetics), Moscow: Nauka, 1967.
18. Rozovskii, A.Ya., Kipnis, M.A., Volnina, E.A., Lin, G.I., and Samokhin, P.V., *Kinet. Katal.*, 2007, vol. 48, no. 5, p. 750 [*Kinet. Catal.* (Engl. Transl.), vol. 48, no. 5, p. 701].
19. Rozovskii, A.Ya., Kipnis, M.A., Volnina, E.A., Lin, G.I., and Samokhin, P.V., *Kinet. Katal.*, 2004, vol. 45, no. 4, p. 654 [*Kinet. Catal.* (Engl. Transl.), vol. 45, no. 4, p. 618].
20. Zhilyaeva, N.A., Volnina, E.A., Shuikina, L.P., and Frolov, V.M., *Neftekhimiya*, 2000, vol. 40, no. 6, p. 422 [*Pet. Chem.* (Engl. Transl.), vol. 40, no. 6, p. 383].
21. Bi Yushui and Lu Gongxuan, *Appl. Catal., B*, 2003, vol. 41, p. 279.
22. Kiss, J.T. and Gonzalez, R.D., *J. Phys. Chem.*, 1984, vol. 88, p. 892.
23. Kiss, J.T. and Gonzalez, R.D., *J. Phys. Chem.*, 1984, vol. 88, p. 898.
24. Arnby, K., Törncrona, A., Andersson, B., and Skoglundh, M., *J. Catal.*, 2004, vol. 221, p. 252.
25. Arnby, K., Assiks, J., Carlsson, P.-A., Palmqvist, A., and Skoglundh, M., *J. Catal.*, 2005, vol. 233, p. 176.
26. Skoglundh, M., Thormählen, P., and Andersson, B., *Top. Catal.,* 2004, vol. 30/31, p. 375.
27. Subbotin, A.N., Gudkov, B.S., and Yakerson, V.I., *Izv. Akad. Nauk, Ser. Khim.*, 2000, no. 8, p. 1379.
28. Kahlich, M.J., Gasteiger, H.A., and Behm, R.J., *J. Catal.*, 1997, vol. 171, p. 93.
29. Galletti, C., Fiorot, S., Specchia, S., Saracco, G., and Specchia, V., *Top. Catal.*, 2007, vol. 45, p. 15.
30. Satterfield, Ch.N., *Heterogeneous Catalysis in Practice*, New York: McGraw-Hill, 1980.
31. Karavaev, M.M., Zasorin, A.P., and Kleshchev, N.F., *Kataliticheskoe okislenie ammiaka* (Catalytic Oxidation of Ammonia), Moscow: Khimiya, 1983.
32. Cant, N.W., Hicks, P.C., and Lennon, B.S., *J. Catal.*, 1978, vol. 54, p. 372.
33. Aßmann, J., Crihan, D., Knapp, M., Lundgren, E., Löffler, E., Muhler, M., Narkhede, V., Over, H., Schmid, M., Seitsonen, A.P., and Varga, P., *Angew. Chem., Int. Ed. Engl.*, 2005, vol. 44, p. 917.
34. Goodman, D.W., Peden, C.H.F., and Chen, M.S., *Surf. Sci.*, 2007, vol. 601, p. L124.
35. Schubert, M.M., Kahlich, M.J., Gasteiger, H.A., and Behm, R.J., *J. Power Sources,* 1999, vol. 84, p. 175.
36. Kurkina, E.S. and Semendyaeva, N.L., *Kinet. Katal.,* 2005, vol. 46, no. 4, p. 485 [*Kinet. Catal.* (Engl. Transl.), vol. 46, no. 4, p. 453].